



**RADAR CROSS SECTION SIMULATION AND ANALYSIS OF A SMALL
DRONE MODEL BY THE HELP OF PREDICS TOOL**

Caner Özdemir ^{*1}

¹Mersin University, Engineering Faculty, Department of Electrical-Electronics Engineering, Mersin, Turkey,
cozdemir@mersin.edu.tr

ABSTRACT

In this paper, we examine the radar cross section (RCS) merits of a small drone model by simulating and assessing the RCS simulation of it by the help of reliable simulator tool of Predics. The analysis and assessment of RCS merit of the Drone model is explored via series of angle-diverse and frequency-diverse numerical RCS simulations. Also, RCS maps of the drone model is also constructed for few frequencies of interest to quickly observe the high RCS look-angles. The RCS simulation results suggest that the RCS of this drone model can reach to 2 m² for S-band microwave frequencies; therefore, it can easily be visible for a nominal radar at a reasonably far distance for the radar. It is also concluded from the RCS results that the RCS variation do not change dramatically for both elevation and horizontal look-angles.

Keywords: Radar Cross Section, Drone RCS calculation, Radar Visibility, RCS simulation

* Corresponding Author

1. INTRODUCTION

Recently, the number of different drone types that are being used in many usages have been expansively amplified due to rising demand from both military and civil institutions (Vinogradov, *et al.*, 2018). The use of drones for leisure and specialized usages may cause personal and government concerns regarding the safety of people. Furthermore, the offensive use of drones as terrorist attacks has become a growing concern in parallel to the increasing number of drones. So, it becomes very vital to detect and also make them useless before succeeding their missions to circumvent possible fatalities and injuries.

Many techniques have been used for the detection of drones. These include visual techniques (Rozantsev, *et al.*, 2017), acoustic techniques (Kim, *et al.*, 2017) and electromagnetic (i.e. radar) techniques (Hoffmann, *et al.*, 2016). Among them, it is no doubt that radar-based methods offer the most reliable detection performance compared to other techniques. While radar hardware can be used to detect the drones, the question becomes if the drones can be sensed at a fairly safe distance from the radar based on their radar cross section (RCS) values. Therefore, there is a quite much of interest in knowing the RCS values of drones to assess their visibility in a nominal radar.

In this work, we offer a study for calculating and examining the RCS of a drone model that is very common for personal leisure usages. The RCS calculation is performed by the recently developed RCS simulation and analysis software called Predics (Özdemir *et al.*, 2014a; Özdemir *et al.*, 2014b).

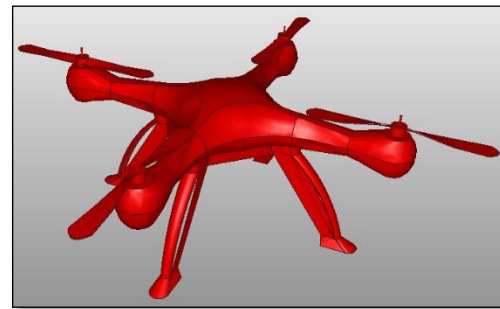
2. RCS SIMULATION OF THE DRONE

2.1. The Drone model

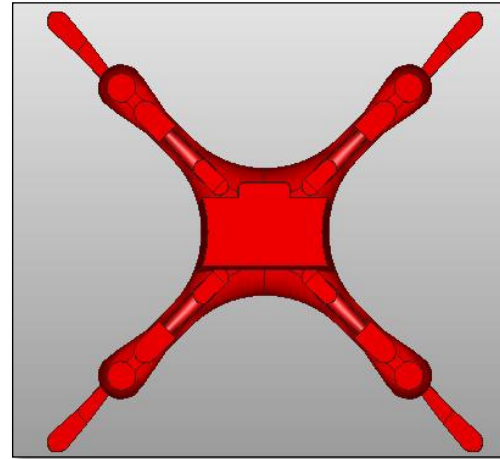
The drone model used in Predics simulation is given in Fig.1. The perspective view of the drone model is given Fig.1(a). The bottom view of the model is as viewed in Fig. 1(b). The side view of the drone model is given in Fig. 1(c). The dimensions of the model are 378 mm, 382 mm, and 165 mm in x-axis, y-axis and z-axis (height), respectively. The model's material is taken as to be perfect electric conductor (PEC).

2.2. RCS simulation by the help of Predics

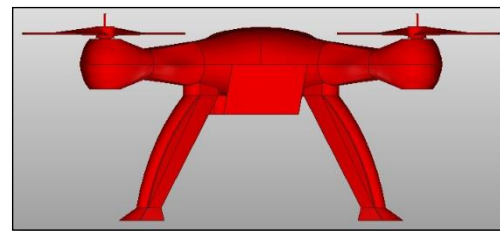
RCS simulation of the drone model has been carried out by the Predics simulator (Özdemir *et al.*, 2014a; Özdemir *et al.*, 2014b). Predics is a fast and effective simulation tool for the reliable calculation of RCS from electrically large and complex-shaped targets at 1 GHz and beyond frequencies. The RCS simulation screen of the drone model can be observed in Fig. 2.



(a)



(b)



(c)

Fig. 1. Small drone model: (a) Perspective view, (b) Bottom view, and (c) side view

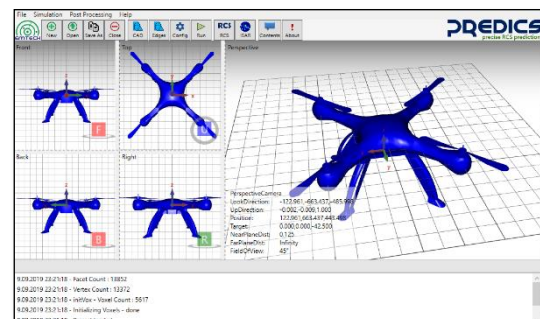


Fig. 2. Predics simulation screen for the drone model

To depict the RCS characteristics of the drone model, various simulations were performed. Firstly, angular RCS variation for a fixed frequency was done.

Then, angular RCS-map plot simulation was accomplished to see the RCS variation of the model with respect to look-angles in a single snap-shot. Furthermore, the frequency RCS variation of the drone model for some fixed look-angles were also done.

2.2.1. RCS variation over angles

In the first simulation, horizontal monostatic RCS variation for a static frequency of 10 GHz has been explored. The detailed simulation parameters are given in Fig. 3.

pRediCS - Simulation Configuration

Threads
 Number of CPU Threads to Use Use CUDA GPU

Method
 PO PO + SBR PO + SBR + PTD
 Wedge Angle (Degree)

Units
 Inch cm meter mm mile

Simulation Mode
 RCS Simulation 2D ISAR Simulation 3D ISAR Simulation

Options
 Ray Density rays, λ Max. Bounce #

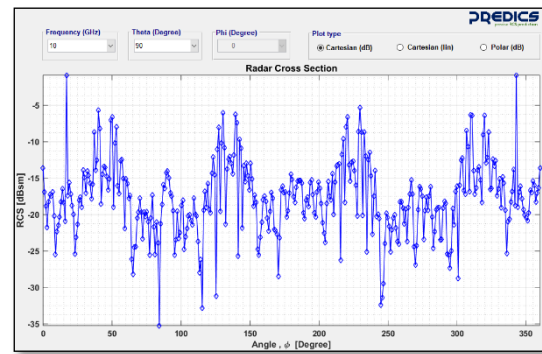
RCS Simulation Options

Frequencies
 Start (GHz) Stop (GHz) Step

Observation Angles
 Use Theta, Phi EL, AZ
 Theta or EL Range (Degree)
 Start Stop Step
 Phi or AZ Range (Degree)
 Start Stop Step

Fig. 3. Simulation parameters for the horizontal angular RCS simulation

The resultant RCS variation over horizontal angles are presented for different polarization excitations in Fig. 4. In Fig 4(a), RCS variation over horizontal angles at a fixed elevation angle of 0° and the fixed frequency of 10 GHz are given for vertical-vertical (VV) [drawn as blue] polarization. As clear from Fig. 4(a), RCS can be as much as 2.83 dBsm (i.e., 1.9 m²) for the look angle of 17° and 2.23 dBsm (i.e., 1.6 m²) for the look angle of 343°. In Fig 4(b), RCS variation over horizontal angles at a fixed elevation angle of 0° and the fixed frequency of 10 GHz are given for horizontal-horizontal (HH) [drawn as red] polarization. As seen from Fig. 4(b), RCS can be as much as -1 dBsm (i.e., 0.78 m²) for the look angle of 17° and -1.3dBsm (i.e., 0.73 m²) for the look angle of 343°.



(a)



(b)

Fig. 4. Horizontal angles RCS simulation results: (a) VV, and (b) HH

2.2.2. Angular RCS MAPs of the drone

As the second simulation, two-dimensional (2D) angle simulation over horizontal and elevation angles were carried out to map the monostatic RCS variation over angles for a static frequency of 8 GHz in a single view. The detailed simulation parameters are given in Fig. 5.

The resultant 2D RCS maps for the VV and HH polarizations are plotted in Fig. 6(a) and Fig. 6(b), respectively. In can be observed from the figure that the RCS value is fluctuating over angles; but do not offer a superior peak or hollow as a whole. This is kind of expected since the geometry of the drone is somewhat a spherical-like shape.

pRediCS - Simulation Configuration

Threads
 Number of CPU Threads to Use Use CUDA GPU

Method
 PO PO + SBR PO + SBR + PTD
 Wedge Angle (Degree)

Units
 Inch cm meter mm mile

Simulation Mode
 RCS Simulation 2D ISAR Simulation 3D ISAR Simulation

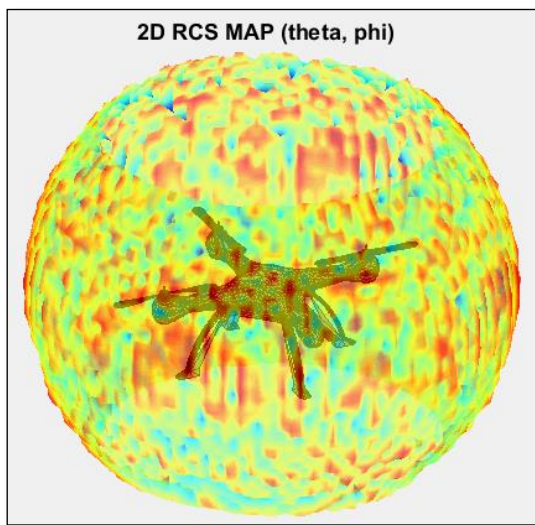
Options
 Ray Density rays, λ Max. Bounce #

RCS Simulation Options

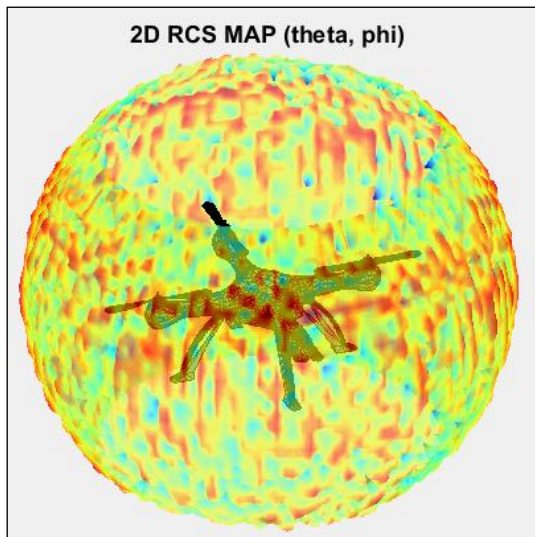
Frequencies
 Start (GHz) Stop (GHz) Step

Observation Angles
 Use Theta, Phi EL, AZ
 Theta or EL Range (Degree)
 Start Stop Step
 Phi or AZ Range (Degree)
 Start Stop Step

Fig. 5. Simulation parameters for 2D angular RCS-map simulation



(a)



(b)

Fig. 6. 2D RCS maps at 8 GHz for (a) VV and (b) HH polarizations

2.2.2. RCS variation over frequencies

As the last study, monostatic RCS variation over

frequencies for the look angle of 0° elevation and 0° & 90° horizontal angles has been tested. The detailed parameters for this particular simulation are given in Fig. 7. As obvious from Fig.7, the frequency is altered from 1 GHz to 10 GHz for a total of 100 distinct frequency values.

pRediCS - Simulation Configuration

Threads
 Number of CPU Threads to Use Use CUDA GPU

Method
 PO PO + SBR PO + SBR + PTD
 Wedge Angle (Degree)

Units
 Inch cm meter mm mile

Simulation Mode
 RCS Simulation 2D ISAR Simulation 3D ISAR Simulation

Options
 Ray Density rays λ Max. Bounce #

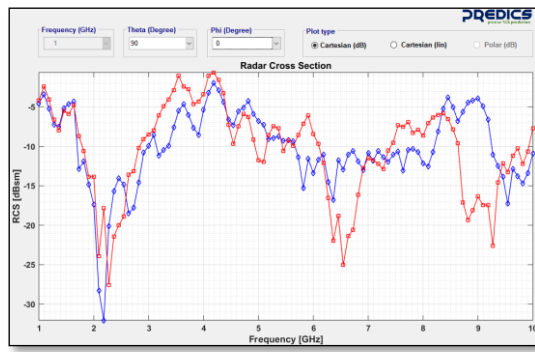
RCS Simulation Options

Frequencies
 Start (GHz) Stop (GHz) Step

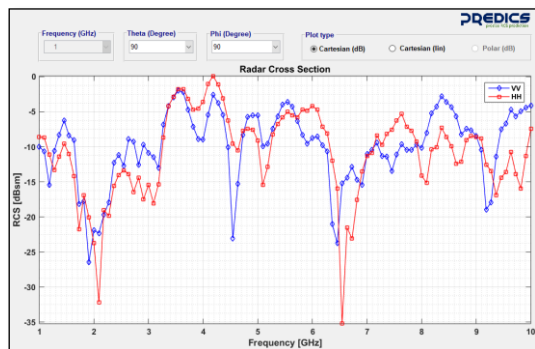
Observation Angles
 Use Theta, Phi EL, AZ
 Theta or EL Range (Degree)
 Start Stop Step
 Phi or AZ Range (Degree)
 Start Stop Step

Fig. 7. Simulation parameters for the RCS simulation of frequency variation

In Fig. 8(a) and 8(b), RCS variation over frequencies for the fixed elevation angle of 0° and the fixed horizontal angles of 0° and 90° are presented, respectively. In Fig. 8(a), the monostatic RCS frequency variation of the drone model and fixed elevation angle of 0° and the fixed horizontal angle of 0° is drawn. This plot is for the VV polarization [drawn as blue] and HH polarization [drawn as red]. In an analogous manner, in Fig. 8(b), the similar RCS plots are supplied for the horizontal angle of 90° . As seen from both graphs, the RCS values are fluctuating with respect to frequency.



(a)



(b)

Fig. 8. RCS frequency variation for the fixed elevation angle of 0° and the fixed horizontal angles of (a) 0° , and (b) 90° : VV-polarization case [blue], (b) HH-polarization case [red]

3. CONCLUSION

In this paper, we have supplied a numerical analysis of RCS from a small drone model to evaluate its visibility feature in a nominal radar. The reliable high-frequency RCS simulator code; Predics has been exploited to perform the RCS simulation and the resultant analyses. Using the Predics tool, both the angle variation and the frequency variation monostatic RCS simulations of the drone model have been carried out. Results suggested that RCS values can reach to 2 m^2 for microwave frequencies. Therefore, this model can easily be sensed and detected by a generic radar.

ACKNOWLEDGEMENTS

This work was supported by Mersin University Scientific Research Unit under Project No. 2015-TP3-1160

REFERENCES

- Hoffmann, F., Ritchie, M., Fioranelli, F., Charlish, A. and Griffiths, H. (2016) "Micro-Doppler based detection and tracking of UAVs with multistatic radar," *IEEE Radar Conference*, 1–6.
- Kim, J., Park, C., Ahn, J., Ko, Y., Park, J., and Gallagher, J. C. (2017) "Real-time UAV sound

detection and analysis system," *IEEE Sensors Applications Symposium*, 1–5.

Rozantsev, A., Sinha, S., Dey, D., and Fua, P. (2017) "Flight Dynamics based Recovery of a UAV Trajectory using Ground Cameras," *CVPR17*, 2482-2491.

Özdemir, C., Yılmaz, B., and Kırık, Ö. (2014a), "pRediCS: A new GO-PO based ray launching simulator for the calculation of electromagnetic scattering and RCS from electrically large and complex structures," *Turkish Journal of Electrical Engineering & Computer Sciences*, Vol. 22, 1255 – 1269

Özdemir, C., Yılmaz, B., Kırık, Ö., Sütcüoğlu, Ö. (2014b), "A Fast and Efficient RCS Calculation and ISAR Image Formation Tool: pRediCS", *10th European Conference on Synthetic Aperture Radar (EUSAR 2014)*, Berlin.

Vinogradov, E., Kovalev, D.A. and Pollin, S. (2018) "Simulation and Detection Performance Evaluation of a UAV-mounted Passive Radar", *The 29th Annual IEEE International Symposium on Personal, Indoor and Mobile Radio Communications (IEEE PIMRC 2018)*, Bologna, 1185-1191.